

Energy analysis of size-dependent elastic properties of ZnO nanofilms using atomistic simulations

Guoxin Cao and Xi Chen

Columbia Nanomechanics Research Center, Department of Civil Engineering and Engineering Mechanics, Columbia University, New York, New York 10027-6699, USA

(Received 8 January 2007; revised manuscript received 4 August 2007; published 5 October 2007)

The size dependence of elastic modulus of ZnO nanofilms is investigated by using atomistic simulations. The strain energy and elastic stiffness of the surface and interior atomic layers, as well as interlayer interactions, are decoupled. The surface stiffness is found to be much lower than that of the interior layers and bulk counterpart, and with the decrease of film thickness, the residual tension-stiffened interior atomic layers are the main contributions of the increased elastic modulus of nanofilms.

DOI: [10.1103/PhysRevB.76.165407](https://doi.org/10.1103/PhysRevB.76.165407)

PACS number(s): 62.20.Fe, 62.20.Dc, 68.60.Bs, 71.15.Pd

INTRODUCTION

Due to high surface-to-volume ratios, the mechanical properties of nanowires and nanofilms are distinct with respect to their bulk forms.¹⁻⁶ Among them, ZnO is becoming an important component in the next-generation nanoelectromechanical systems and biomedical devices, thanks to its semiconducting, piezoelectric, and biocompatible properties.⁷

In order to fulfill their promising applications, the size dependence of mechanical properties of nanowires or nanofilms needs to be sufficiently understood. Cuenot *et al.*² reported that the measured elastic moduli of Ag and Pb nanowires increase dramatically with decreasing diameters. However, studies on Cr and Si nanocantilevers showed that their moduli sharply decrease with the reduction of diameters.^{3,4} By contrast, the results given by Wong *et al.*⁵ and Wu *et al.*⁶ showed that the moduli of SiC and Au nanowires are essentially insensitive to the variation of wire diameter. For ZnO, Chen *et al.*¹ reported that the elastic modulus of ZnO nanowire is increasing significantly with decreasing diameter, whereas other groups' results showed that there is no obvious size effect on the elastic modulus of ZnO.⁸⁻¹¹

Theoretical analyses were also employed to extract the mechanical responses of nanostructures, which include atomistic simulations¹²⁻²⁰ and continuum modeling.^{1,21,22} The molecular simulations of Porezag *et al.*¹⁶ reported that Pt and Au nanowires become more compliant when the nanowire is thinner. Atomistic studies by Kulkarni *et al.*^{12,17} showed that with the increase of the diameter of ZnO nanowire, both the elastic modulus and ultimate tensile strength decrease until they approach the bulk properties. The *ab initio* simulations by Zhang and Huang²⁰ showed that the Young's modulus of ZnO nanofilm increases exponentially as the film thickness is reduced.

In essence, the size dependence of nanomaterials arises from the surface: the surface atoms have different coordination numbers, which cause the bonds to relax so as to decrease the system potential energy. In almost all previous models of explaining the size effect of elasticity (including ZnO and other materials), it was simply assumed that the trend of surface elastic modulus must be consistent with the size effect and the core has the same elastic modulus as the

bulk material.^{1,17-19} For example, Sun *et al.*²³ identified an empirical relationship between the bond length and energy, and they assumed that the surface modulus should be higher than its bulk counterpart. Inspired by such stiffening effect of surface, various continuum models were developed. Bazant and Guo²⁴ divided a metallic film into a boundary layer and an inner core, and the stress-strain relationship of the entire film equals the average of both parts. In this model, they argued that the boundary layer causes significantly elevated yield strength at smaller film thickness. Recently, Chen *et al.*¹ employed a core-shell composite model to divide a ZnO nanowire into a cylindrical core having an elastic modulus the same as that of the bulk and a coaxial shell having a higher surface modulus (about 1.5 times of bulk ZnO). However, the key assumption that the surface of nanostructure is stiffer than the core and the bulk counterpart is not yet validated. In terms of ZnO, it was argued that as the bond lengths at the surface contract up to 5%–8%, the surface should contract and thus the surface tension should increase the surface modulus especially for thinner nanowires,¹ which was believed to be the mechanism of size-dependent elastic properties in ZnO. However, there was no explicit evidence to show that the contraction of bond length at the surface causes the surface contraction, nor evidence to show that the surface is stiffer than the bulk.

In this paper, a comprehensive atomistic investigation is carried out to explore the surface elastic modulus and its quantitative contribution to the overall stiffness of the nanofilm, as well as to explain the mechanism of the size dependence of elastic modulus. We focus on ZnO nanofilms instead of nanowires, since the nanofilm allows us to focus on the intrinsic film thickness effect (unlike nanowire which involves interactions between two pairs of surface orientations that are coupled with each other); in addition, the atoms at the corner of a nanowire have a very high potential energy which may cause partial melting of the corner and thus influence the elastic property of nanostructure obtained from theoretical calculations.

COMPUTATION METHOD

The strain energies of surface and interior atomic layers of ZnO film are computed by using molecular mechanics (MM) method, where the initial structures are optimized with the

COMPASS force field, the first and only *ab initio* force field that enables an accurate and simultaneous prediction of various gas-phase and condensed-phase properties of organic and inorganic materials.^{25–27} The force field is validated via sample computations (e.g., phase transformation from wurtzite to graphitic structure upon large deformation) and compared with literature.^{12,28} The undeformed lattice constants are $a=3.249$ Å and $c=5.206$ Å. The bulk ZnO is studied using a periodical computational cell with size of $1.122 \times 5.227 \times 0.972$ nm³, whose elastic modulus is found to be independent of the cell size via a convergence study. To simulate ZnO nanofilm, an initial computational cell of $1.122 \times 5.227 \times 50$ nm³ is employed; due to surface relaxation, the in-plane cell dimensions (in the x and y directions) are determined by optimization, which are slightly dependent on the film thickness t . The periodical boundary conditions are applied in both in-plane directions, whereas the periodic length in the z direction (out of plane) is much larger than t . The film thickness varies from about 0.8 to 8.0 nm.

The elastic deformation is calculated under uniaxial loading (in the y direction) within $\pm 0.5\%$ of strain. The system potential energy (U_{tot}) is the summation of energy of each atomic layer and the interaction energy between any pair of atomic layers:

$$U_{tot} = \sum_{i=1}^n U_i + \sum_{i=1}^{n-1} U_{i,i+1} + \sum_{|i-j|>1} U_{i,j}, \quad (1)$$

where, in the computational cell containing n layers of atoms, U_i is the potential energy of the i th intralayer of atoms and $U_{i,j}$ is the interaction energy between the i th and j th atomic layers. Upon axial loading, U_{tot} will increase, which is related to the variation of each component:

$$\Delta U_{tot} = \sum_{i=1}^n \Delta U_i + \sum_{i=1}^{n-1} \Delta U_{i,i+1} + \sum_{|i-j|>1} \Delta U_{i,j}. \quad (2)$$

When ΔU_{tot} is fitted as a polynomial function of strain (ε), the quadratic term is dominant. The effective elastic stiffness of the nanofilm or bulk is

$$\tilde{E}_{tot} = \left. \frac{1}{S} \frac{\partial^2 \Delta U_{tot}}{\partial \varepsilon^2} \right|_{\varepsilon=0}, \quad (3)$$

where S is the area of the specimen in the x - y plane. The effective elastic modulus of the specimen can be further calculated by $E_{tot} = \tilde{E}_{tot}/t$. While there is no net stress in the undeformed nanofilm or bulk, due to the strong coupling among surface, intralayer and interlayer bond deformation, residual stress (e.g., surface stress in nanofilm) may exist in any component, intralayer or interlayer. For interlayer or intralayer, the effective residual stress is the variation of strain energy per unit area with respect to strain:

$$\tilde{\sigma}_i = \left. \frac{1}{S} \frac{\partial \Delta U_i}{\partial \varepsilon} \right|_{\varepsilon=0} \quad (i = 1 \sim n) \quad \text{and}$$

$$\tilde{\sigma}_{i,j} = \left. \frac{1}{S} \frac{\partial \Delta U_{i,j}}{\partial \varepsilon} \right|_{\varepsilon=0} \quad (i \neq j), \quad (4)$$

respectively. The intralayer residual stresses (including surface stress when $i=1$ or n in nanofilm) balance with interlayer residual stresses, such that the net stress of the film or bulk is zero. For each component, intralayer and interlayer,

$$\begin{aligned} \tilde{E}_i &= \left. \frac{1}{S} \frac{\partial^2 \Delta U_i}{\partial \varepsilon^2} \right|_{\varepsilon=0} \quad (i = 1 \sim n) \quad \text{and} \\ \tilde{E}_{i,j} &= \left. \frac{1}{S} \frac{\partial^2 \Delta U_{i,j}}{\partial \varepsilon^2} \right|_{\varepsilon=0} \quad (i \neq j) \end{aligned} \quad (5)$$

are their effective elastic stiffness, respectively, with unit of [pressure] [length] (same as the effective residual stresses). If the intralayers were parallel plates without interactions, then \tilde{E}_{tot} would equal the summation of intralayer stiffness. Due to the coupled bond deformation between intralayers and interlayers, however, the effective elastic stiffness of the entire film is higher:

$$\tilde{E}_{tot} = \sum_{i=1}^n \tilde{E}_i + \sum_{i=1}^{n-1} \tilde{E}_{i,i+1} + \sum_{|i-j|>1} \tilde{E}_{i,j}. \quad (6)$$

To simplify the model, since $\Delta U_{i,i+1} > \Delta U_{i,j}$ ($|i-j| > 1$), the contributions of the nearest-neighbor interlayer interaction are more important than that of the non-nearest neighbors. The overall film stiffness can be based on the intralayers and nearest-neighbor interlayers:

$$\tilde{E}_{tot} \approx \sum_{i=1}^n \tilde{E}_i + w \sum_{i=1}^{n-1} \tilde{E}_{i,i+1}, \quad (7)$$

where w is a factor that underpins the total interlayer stiffness based on that of the nearest-neighbor interactions, which will be fitted from MM simulations.

RESULTS AND DISCUSSION

The elastic moduli of ZnO nanofilms ($E_{tot}^{film} \equiv E_f$) are shown in Fig. 1 and compared with that of the bulk. The computed elastic modulus of bulk ZnO, $E_{tot}^{bulk} \equiv E_b = 162$ GPa, is close to that found in the literature.¹⁷ Note that E_f increases exponentially as t decreases, a trend that agrees well with that reported in previous experiment of ZnO nanowires¹ and *ab initio* simulations on ZnO nanoplates.²⁰ When t is large, E_f approaches E_b .

Figures 2(a) and 2(b) show the strain energy curves of representative layers of bulk and nanofilms, respectively, where $i=1$ is counted from the surface of the nanofilm. To simplify the results, in Fig. 2(b), we only show the results of nanofilm with $t=1.75$ nm ($n=12$), and the general characteristics remained for other film thicknesses.

For bulk ZnO [Fig. 2(a)], the values of ΔU_i^{bulk} and $\Delta U_{i,j}^{bulk}$ are essentially the same for any i . From the first derivatives, the effective intralayer residual stress ($\tilde{\sigma}_i^{bulk}$) is positive, and that of interlayer ($\tilde{\sigma}_{i,j}^{bulk}$) is negative. In order to balance the intralayer residual tension, an interlayer residual compres-

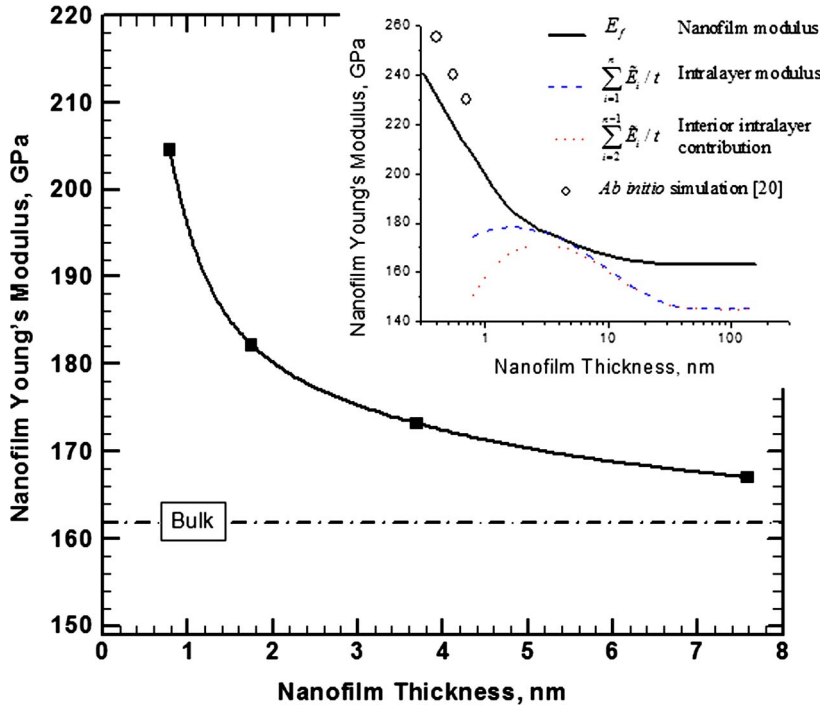


FIG. 1. (Color online) The elastic modulus of bulk and ZnO films with different film thicknesses. The fitting from MM simulations (including film modulus and intralayer contributions) is given in inset, which agrees well with that of Ref. 20.

sion is developed which is caused by the coupling between intralayer and interlayer. The summation of all intralayer and interlayer residual stresses should be zero (note that ΔU_{tot}^{bulk} is symmetric about $\varepsilon=0$ at small strain).

From second derivatives, the effective bulk intralayer stiffness is $\tilde{E}_i^{bulk}=23.6$ GPa nm, and its nearest-interlayer stiffness is $\tilde{E}_{i,i+1}^{bulk}=18.3$ GPa nm. On the other hand, from Eq. (3), $\tilde{E}_{tot}^{bulk}=\tilde{E}_{tot}^{bulk}t=157.6$ GPa nm (since $n=6$ and $t=0.972$ nm); thus, the weighting factor $w\approx 0.15$, which means that non-nearest-neighbor interactions have an opposite overall effect with respect to the nearest neighbors, together, the interlayer contribution is much smaller than that of the intralayer: the intralayer stiffness accounts for about 90% of the overall bulk ZnO stiffness.

From Fig. 2(b), the film surface residual stress is compressive ($\tilde{\sigma}_1^{film}<0$), which is caused by surface expansion and such characteristic also holds for other film thicknesses investigated. This can be confirmed by the undeformed film lengths of computational cell in the y direction (after cell optimization) of $L^{film}=5.261, 5.245, 5.234,$ and 5.231 nm, as the film encompasses 6, 12, 24, and 48 layers of atoms, respectively, which are all longer than that of the bulk, $L^{bulk}=5.227$ nm. Apparently, the smaller the t , the longer the film; similar trends are observed in the x direction. Since the surface atoms have imperfect coordination numbers, both surface bond length and bond angle are adjusted; although the bond length is reduced, the bond angle adjustment leads to a moderate surface expansion. Due to the constraint of remaining layers, the surface layer cannot fully expand to its desired intrinsic (fully relaxed) length, which not only releases the original intralayer tensile stress of bulk ZnO but also creates a residual compressive surface stress. The surface stress must be balanced by that in the interior: from the trends of ΔU_i^{film} ($i=2, 3, 4$) in Fig. 2(b), the intralayers below the surface have residual tension. On the other hand, all

nearest-neighbor interlayer residual stresses, $\tilde{\sigma}_{1,2}^{film}, \tilde{\sigma}_{2,3}^{film}, \tilde{\sigma}_{3,4}^{film}$, etc., are negative.

For nanofilms with varying t , the effective intralayer and interlayer stiffnesses are shown in Fig. 3. The effective surface stiffness ($\tilde{E}_1^{film}=5.0-9.7$ GPa nm) is much lower than \tilde{E}_i^{bulk} , and it decreases with the increase of t . All other intralayer stiffnesses are higher than \tilde{E}_i^{bulk} : \tilde{E}_2^{film} sharply increases to 26.8–29.4 GPa nm, \tilde{E}_3^{film} is slightly higher than \tilde{E}_2^{film} , and \tilde{E}_4^{film} is essentially the same as \tilde{E}_3^{film} . With the increase of i , the increasing \tilde{E}_i^{film} soon approaches a constant once the bond structures of subsequent intralayers are converged. As t gets large, the intralayer stiffness slightly decreases and converges to that of the bulk. For interlayers, $\tilde{E}_{i,i+1}^{film}$ show an increasing trend and they also converge to the value of bulk material as t increases.

Unlike the assumption commonly adopted in literature, the ZnO surface layer is the most compliant among all intralayers (Fig. 3), and its stiffness is even much lower than that of the bulk. Thus, the conventional continuum models based on the surface stiffening effect^{1,18} become invalid for ZnO nanofilms. The higher modulus of ZnO nanofilm with smaller thickness is indeed due to the stiffening effect of intralayers below the surface, where the bond structure variation in nanofilms leads to residual tension in subsurface layers, which, through nonlinear constitutive relationships, stiffens the interior intralayers and also the nanostructure.

When t increases, L^{film} decreases which leads to a less relaxed surface layer and higher compressive surface residual stress; subsequently, the effective surface elastic stiffness becomes lower. In order to offset the compressive surface stress, the interior intralayers develop residual tension. Since the stiffened interior layers are more prominent than the surface, E_f becomes larger than E_b . With the increase of t , more interior atomic layers are involved and therefore their

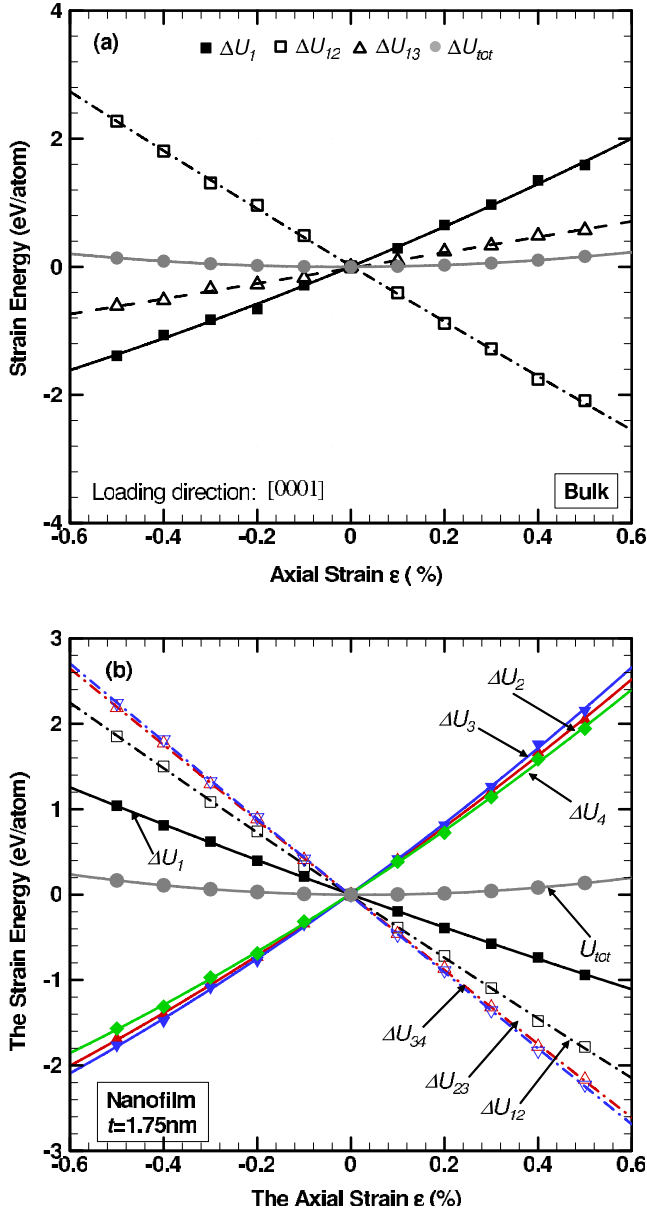


FIG. 2. (Color online) The strain energy of intralayers and interlayers with respect to axial strain: (a) ZnO bulk and (b) ZnO nanofilm with $t=1.75$ nm.

residual tension becomes smaller, leading to smaller intralayer stiffness (Fig. 3). Subsequently, the thinner film has a higher elastic modulus, i.e., the size effect (Fig. 1). The above trend is not well preserved for the thinnest film in this study ($t=0.8$ nm), since it has lower \tilde{E}_2^{film} and \tilde{E}_3^{film} (when compared with thicker nanofilms) but a higher E_f —this is possibly caused by the interaction between two film surfaces due to the very small t . Such interaction further adjusts the atomic coordinates, leading to a larger contribution of the interlayer stiffness.

From the above analysis, the ZnO nanofilm can be modeled as a composite film including a surface layer with a low stiffness and interior intralayers with higher stiffness, plus contributions from the interlayer. The nanofilm elastic stiffness is then

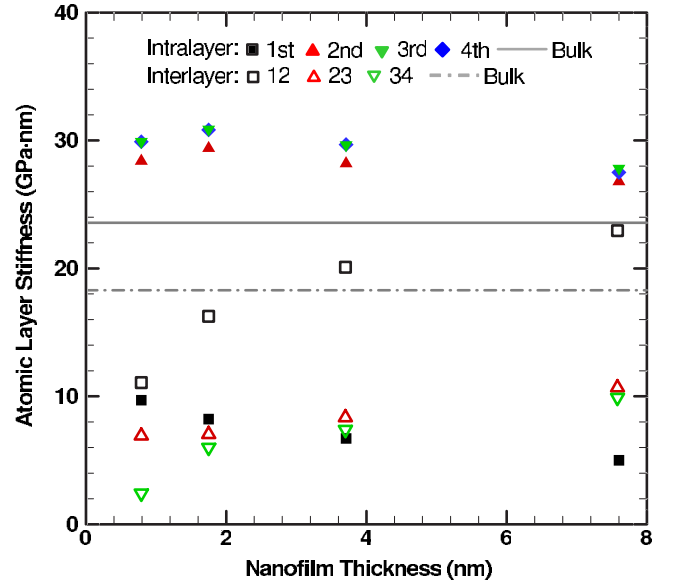


FIG. 3. (Color online) The intralayer and interlayer stiffnesses of ZnO bulk and nanofilms.

$$\tilde{E}_f = E_f t = 2\tilde{E}_s + 2 \sum_{i=2}^{n/2} \tilde{E}_i + \tilde{E}_{int}. \quad (8)$$

Here, t is a function of the number of atomic layers n . \tilde{E}_s is the surface elastic stiffness and \tilde{E}_i is the interior intralayer stiffness of the i th layer, respectively. $\tilde{E}_{int} = w \sum_{i=1}^{n-1} \tilde{E}_{i,i+1}$ is the interlayer stiffness. The effects of residual stresses are implicitly embedded in \tilde{E}_s , \tilde{E}_i , and \tilde{E}_{int} , which depend on the film thickness. The model in Eq. (8) can be readily extended to other nanofilms, although it should be noted that for different materials, the contributions of surface layer, interior intralayer, and interlayers may be different, which may lead to different size dependences of E_f .

Specified for ZnO, the following results can be fitted from MM simulations: the film thickness $t=0.162n(1-n^{-0.95})$ (nm), the surface elastic stiffness $\tilde{E}_s = \tilde{E}_1^{film} = 4.0 + 7.1e^{-n/26}$ (GPa nm), and the interlayer stiffness $\tilde{E}_{int} = n[4.1(e^{-0.214(n-7.28)} - e^{-0.012(n-7.28)}) + 2.3]$ (GPa nm). When $i=2 \sim n/2$, the interior intralayer stiffness is $\tilde{E}_i = \tilde{E}_i^{film} = 24 + 8.0e^{-n/61.1} - 900 \cdot e^{-(19.33+n/18) \cdot i/n}$ (GPa nm). The nanofilm modulus (Fig. 1) is roughly $E_f = 162 + 139e^{-n/3.39} + 23.5e^{-n/31.2}$ (GPa). The fitting has accuracy over 97%, and as n gets very large, the trends of the above fitting equations agree well with bulk ZnO simulations. The results of the fitted E_f , $\sum_{i=1}^n \tilde{E}_i/t$, and $\sum_{i=2}^{n-1} \tilde{E}_i/t$ are given in the inset of Fig. 1. When t is relatively large, there are many interior intralayers, and thus the contribution of the weakened surface to the overall stiffness can be neglected. In all cases, the interior intralayer stiffness $\sum_{i=2}^{n-1} \tilde{E}_i$ accounts for the most part of \tilde{E}_f ; the remaining difference is the minor interlayer contribution. We note that according to the inset of Fig. 1, E_f obtained from this study (line) also agrees well with that obtained from previous quantum mechanics simulations²⁰ (open sym-

bols) when the film is very thin, and the mechanism of size-dependent elasticity of ZnO is elucidated in this paper.

CONCLUSION

To summarize, a strain energy analysis for ZnO nanofilms under axial loading is carried out using MM. The study focuses on decoupling the strain energies of the surface atomic layer, interior intralayers, and interlayers, from the derivatives of which the effective residual stresses and elastic stiffness of each component layer are derived. It is found that the elastic modulus of ZnO nanofilm increases when the film thickness is reduced. The effective surface elastic stiffness of nanofilm is much lower than that of the interior intralayers and bulk, which is due to the residual compressive stress caused by surface expansion that leads to a weakened sur-

face. By contrast, the interior layers are stiffened by residual tension (which is larger when the film is thinner), resulting in a higher modulus. The present paper focuses on the intrinsic mechanism of the thickness effect of elastic modulus of ZnO films, although elasticity also depends on orientation (such effect will be published elsewhere). The mechanisms found in this paper may provide useful insights for the development of a model explaining the intrinsic size dependence of ZnO nanofilm, where the main contribution comes from the stiffened subsurface intralayers; the general methodology can be extended to other nanostructures.

ACKNOWLEDGMENTS

This work is supported in part by NSF (CMS-0407743 and CMMI-0643726) and in part by Columbia University Academic Quality Fund.

-
- ¹C. Q. Chen, Y. Shi, Y. S. Zhang, J. Zhu, and Y. J. Yan, *Phys. Rev. Lett.* **96**, 075505 (2006).
- ²S. Cuenot, C. Fretigny, S. Demoustier-Champagne, and B. Nysten, *Phys. Rev. B* **69**, 165410 (2004).
- ³S. G. Nilsson, X. Borrisé, and L. Montelius, *Appl. Phys. Lett.* **85**, 3555 (2004).
- ⁴X. Li, T. Ono, Y. Wang, and M. Esashi, *Appl. Phys. Lett.* **83**, 3081 (2003).
- ⁵E. W. Wong, P. E. Sheehan, and C. M. Lieber, *Science* **277**, 1971 (1997).
- ⁶B. Wu, A. Heidelberg, and J. Boland, *Nat. Mater.* **4**, 525 (2005).
- ⁷Z. L. Wang, X. Y. Kong, Y. Ding, P. Gao, W. L. Hughes, R. Yang, and Y. Zhang, *Adv. Funct. Mater.* **14**, 943 (2004).
- ⁸X. D. Bai, P. X. Gao, Z. L. Wang, and E. G. Wang, *Appl. Phys. Lett.* **82**, 4806 (2003).
- ⁹K. Yum, Z. Wang, A. P. Suryavanshi, and M. F. Yu, *J. Appl. Phys.* **96**, 3933 (2004).
- ¹⁰J. Song, X. Wang, E. Riedo, and Z. L. Wang, *Nano Lett.* **5**, 1954 (2005).
- ¹¹H. Ni and X. Li, *Nanotechnology* **17**, 3591 (2006).
- ¹²A. J. Kulkarni, M. Zhou, and F. J. Ke, *Nanotechnology* **16**, 2749 (2005).
- ¹³D. E. Segall, S. Ismail-Beigi, and T. A. Arias, *Phys. Rev. B* **65**, 214109 (2002).
- ¹⁴H. Liang, M. Upmanyu, and H. Huang, *Phys. Rev. B* **71**, 241403(R) (2005).
- ¹⁵V. B. Shenoy, *Phys. Rev. B* **71**, 094104 (2005).
- ¹⁶D. Porezag, T. Frauenheim, T. Kohler, G. Seifert, and R. Kaschner, *Phys. Rev. B* **51**, 12947 (1995).
- ¹⁷A. J. Kulkarni and M. Zhou, *Acta Mech. Sin.* **22**, 217 (2006).
- ¹⁸L. G. Zhou and H. Huang, *Appl. Phys. Lett.* **84**, 1940 (2004).
- ¹⁹K. Gall, J. Diao, and M. L. Dunn, *Nano Lett.* **4**, 2431 (2004).
- ²⁰L. Zhang and H. Huang, *Appl. Phys. Lett.* **89**, 183111 (2006).
- ²¹J. Q. Broughton, C. A. Meli, P. Vashishta, and R. K. Kalia, *Phys. Rev. B* **56**, 611 (1997).
- ²²R. E. Miller and V. B. Shenoy, *Nanotechnology* **11**, 139 (2000).
- ²³C. Q. Sun, B. K. Tay, X. T. Zeng, S. Li, T. P. Chen, J. Zhou, H. L. Bai, and E. Y. Jiang, *J. Phys.: Condens. Matter* **14**, 7781 (2002).
- ²⁴Z. Bazant and Z. Guo, *J. Appl. Phys.* **97**, 073506 (2005).
- ²⁵H. Sun, P. Ren, and J. R. Fried, *Comput. Theor. Polym. Sci.* **8**, 229 (1998).
- ²⁶H. Sun, *J. Phys. Chem. B* **102**, 7338 (1998).
- ²⁷D. Rigby, H. Sun, and B. E. Eichinger, *Polym. Int.* **44**, 311 (1998).
- ²⁸A. J. Kulkarni, M. Zhou, K. Sarasamak, and S. Limpijumnong, *Phys. Rev. Lett.* **97**, 105502 (2006).